Impaired phosphorylation of Na^+-K^+-$2Cl^-$ cotransporter by oxidative stress-responsive kinase-1 deficiency manifests hypotension and Bartter-like syndrome

Shih-Hua Lin[a,b], I-Shing Yu[c], Si-Tse Jiang[d], Shu-Wha Lin[c], Pauling Chu[a], Ann Chen[b], Huey-Kang Sytwu[e], Eisei Sohara[f], Shinichi Uchida[f], Sei Sasaki[f], and Sung-Sen Yang[a,b,1]

[a]Division of Nephrology, Department of Medicine, Tri-Service General Hospital, [b]Graduate Institute of Medical Sciences, and [e]Graduate Institute of Microbiology and Immunology, National Defense Medical Center, Taipei 114, Taiwan; [c]Department of Clinical Laboratory Sciences and Medical Biotechnology, National Taiwan University, Taipei 100, Taiwan; [d]National Laboratory Animal Centre, National Applied Research Laboratories, Taipei 115, Taiwan; and [f]Department of Nephrology, Graduate School of Medicine, Tokyo Medical and Dental University, Tokyo 113-8519, Japan

Edited by Maurice B. Burg, National Heart, Lung, and Blood Institute, Bethesda, MD, and approved September 12, 2011 (received for review May 11, 2011)

Na^+-K^+-$2Cl^-$ cotransporters (NKCCs), including NKCC1 and renal-specific NKCC2, and the Na^+-Cl^- cotransporter (NCC) play pivotal roles in the regulation of blood pressure (BP) and renal NaCl reabsorption. Oxidative stress-responsive kinase-1 (OSR1) is a known upstream regulator of N(K)CCs. We generated and analyzed global and kidney tubule-specific (KSP) OSR1 KO mice to elucidate the physiological role of OSR1 in vivo, particularly on BP and kidney function. Although global $OSR1^{-/-}$ mice were embryonically lethal, $OSR1^{+/-}$ mice had low BP associated with reduced phosphorylated (p) STE20 (sterile 20)/SPS1-related proline/alanine-rich kinase (SPAK) and p-NKCC1 abundance in aortic tissue and attenuated p-NKCC2 abundance with increased total and p-NCC expression in the kidney. KSP-$OSR1^{-/-}$ mice had normal BP and hypercalciuria and maintained significant hypokalemia on a low-K^+ diet. KSP-$OSR1^{-/-}$ mice exhibited impaired Na^+ reabsorption in the thick ascending loop on a low-Na^+ diet accompanied by remarkably decreased expression of p-NKCC2 and a blunted response to furosemide, an NKCC2 inhibitor. The expression of total SPAK and p-SPAK was significantly increased in parallel to that of total NCC and p-NCC despite unchanged total NKCC2 expression. These results suggest that, globally, OSR1 is involved in the regulation of BP and renal tubular Na^+ reabsorption mainly via the activation of NKCC1 and NKCC2. In the kidneys, NKCC2 but not NCC is the main target of OSR1 and the reduced p-NKCC2 in KSP-$OSR1^{-/-}$ mice may lead to a Bartter-like syndrome.

Bartter syndrome | electrolytes | hormone | knockout mice | volume

Recent studies have shown that Na^+-K^+-$2Cl^-$ cotransporters (NKCCs) and the Na^+-Cl^- cotransporter (NCC) play very important roles in the regulation of blood pressure (BP) and extracellular volume. NKCCs consist of ubiquitous NKCC1 and renal-specific NKCC2. NKCC1 can modulate BP through vascular and renal effects (1–4). NKCC2 and NCC are two renal Na^+ cotransporters expressed in the thick ascending limbs (TALs) and distal convoluted tubules (DCTs) of the kidney, respectively, accounting for 20% and 10% of filtered Na^+ reabsorption (5). In human essential hypertension and salt-sensitive or spontaneously hypertensive animal models, activation of NKCC1 and NKCC2 has also been reported to play a pivotal role in the pathogenesis of hypertension (6, 7). In addition, activation of NCC by gene mutations in *WNK1* and *WNK4* leads to an autosomal dominant salt-sensitive hypertension known as pseudohypoaldosteronism type II (PAHII) (8). On the other hand, loss-of-function mutations in the *SLC12A1* and *SLC12A3* genes encoding NKCC2 and NCC can lead to renal salt-wasting hypotension with hypokalemic metabolic alkalosis, known as Bartter syndrome (BS) (9) and Gitelman syndrome (GS) (10), respectively.

In vitro studies have shown that posttranscriptional phosphorylation of NKCC1/2 and NCC plays a crucial role in the regulation of normal transport activity. Oxidative stress-responsive kinase-1 (OSR1) (11) and STE20 (sterile 20)/SPS1-related proline/alanine-rich kinase (SPAK) (12), two downstream substrates of With-No-Lysine kinase (WNK) 1/4, are the upstream phosphorylators of NKCC1/2 and NCC. Threonine or serine residues in their N-terminal conserved domains (T206/96, T211/101, and T224/114 in mouse NKCC1/2; T53, T58 and S71 in mouse NCC) are the phosphorylation sites of OSR1 and SPAK. The docking site on the conserved C-terminal domains of OSR1/SPAK interacts with the RFXV/I motif on the N terminus of NKCC/NCC and then increases NKCC/NCC phosphorylation and function (13–16). We have also reported that increased phosphorylated (p) OSR1/SPAK abundance can enhance p-NCC expression in the PHAII-causing *Wnk4* D561A knock-in mice (17), whereas the reverse is true in the *Wnk4* hypomorphic knockout (KO) mice (18). These findings support that OSR1 and SPAK are important regulators of NKCC and NCC in vivo.

Because OSR1 and SPAK share high homology in their catalytical and regulatory domains and their expression in tissues often overlaps, the creation and analysis of distinct OSR1 or SPAK KO mice is warranted to tease apart the role of each kinase in vivo. For this purpose, we first generated SPAK KO mice and found that $SPAK^{+/-}$ mice exhibited hypotension with decreased p-NKCC1 abundance in aortic tissues and $SPAK^{-/-}$ mice presented a GS phenotype caused by reduced total and p-NCC expression (19). In the present study, we generated global and kidney tubule-specific (KSP) OSR1 KO mice to elucidate the physiological role of OSR1 in vivo (*SI Text* and Figs. S1 and S2). Results to be reported indicate that global $OSR1^{-/-}$ mice were embryonically lethal and $OSR1^{+/-}$ mice had low BP associated with reduced p-SPAK expression and p-NKCC1 abundance in aortic tissue and attenuated p-NKCC2 abundance with increased total and p-NCC expression in the kidney. KSP-$OSR1^{-/-}$ mice manifested Bartter-like syndrome because of impaired NKCC2 phosphorylation and function in the TAL with a compensatory increase in NCC phosphorylation and expression. This study provides in vivo evidence that OSR1 is primarily involved in the regulation of BP and renal tubular Na^+ reabsorption via the phosphorylation of NKCC1 and NKCC2 but not NCC.

Results

Phenotype in Global $OSR1^{+/-}$ and KSP-$OSR1^{-/-}$ Mice. First, we examined BP and electrolyte homeostasis in the global $OSR1^{+/-}$ and KSP-$OSR1^{-/-}$ mice on a normal diet (0.4% Na^+ wt/wt, 1% K^+ wt/wt). Compared with WT littermates, the global $OSR1^{+/-}$ mice had relative hypotension ($P < 0.05$) without serum and urine

Author contributions: S.-H.L. and S.-S.Y. designed research; I.-S.Y. and S.-S.Y. performed research; I.-S.Y., S.-T.J., and S.-W.L. contributed new reagents/analytic tools; S.-H.L., P.C., A.C., H.-K.S., E.S., S.U., S.S., and S.-S.Y. analyzed data; and S.-H.L. and S.-S.Y. wrote the paper.

The authors declare no conflict of interest.

This article is a PNAS Direct Submission.

[1]To whom correspondence should be addressed. E-mail: sungsenyang@hotmail.com.

This article contains supporting information online at www.pnas.org/lookup/suppl/doi:10.1073/pnas.1107452108/-/DCSupplemental.

Table 1. BP and blood and urine biochemistry values in global OSR1$^{+/-}$ mice

Diet	Normal		Low Na$^+$	
Genotype (*n*)	WT (*n* = 12)	OSR$^{+/-}$ (*n* = 12)	WT (*n* = 8)	OSR$^{+/-}$ (*n* = 8)
BP, mmHg				
Systolic	111 ± 6	99 ± 5*	108 ± 7	95 ± 6*
Diastolic	58 ± 4	49 ± 8*	54 ± 4	51 ± 11
Mean	74 ± 4	64 ± 7*	71 ± 5	62 ± 7*
Weight, g	22.8 ± 2.2	21.6 ± 2.3	23.6 ± 3.5	22.1 ± 4.3
Plasma				
PAC, pg/mL	932 ± 413	835 ± 212	1,325 ± 313	1,138 ± 323
PRA, ng·mL·h	6.4 ± 3.0	6.5 ± 2.9	12.2 ± 2.5	10.3 ± 3.5
Na$^+$, mmol/L	157 ± 3	156 ± 2	153 ± 6	154 ± 5
K$^+$, mmol/L	4.3 ± 0.3	4.1 ± 0.3	4.2 ± 0.4	4.3 ± 0.4
Cl$^-$, mmol/L	115 ± 2	113 ± 4	115 ± 2	113 ± 4
Ca^{2+}, mg/dL	9.5 ± 0.2	9.6 ± 0.4	9.3 ± 0.5	9.4 ± 0.6
Mg^{2+}, mg/dL	2.9 ± 0.1	3.1 ± 0.2	3.0 ± 0.3	3.1 ± 0.4
Cr, mg/dL	0.13 ± 0.05	0.12 ± 0.04	0.11 ± 0.08	0.11 ± 0.06
Urine, mL/d	1.77 ± 0.82	1.86 ± 0.73	1.25 ± 0.63	1.23 ± 0.65
Na$^+$, μmol/d	220 ± 56	262 ± 65	53 ± 8	50 ± 10
K$^+$, μmol/d	435 ± 133	520 ± 108	514 ± 155	539 ± 178
Cl$^-$, μmol/d	256 ± 85	306 ± 85	80 ± 22	84 ± 14
Mg^{2+}, mg/d	0.47 ± 0.11	0.50 ± 0.13	0.53 ± 0.21	0.48 ± 0.22
FE_{Na}, %	0.65 ± 0.24	0.68 ± 0.37	0.25 ± 0.09	0.23 ± 0.11
FE_K, %	18.3 ± 6.1	20.2 ± 8.6	20.6 ± 8.2	22.1 ± 9.4
FE_{Cl}, %	0.57 ± 0.12	0.61 ± 0.19	0.21 ± 0.04	0.16 ± 0.05
FE_{Mg}, %	10.5 ± 2.3	10.6 ± 2.5	10.5 ± 2.3	10.6 ± 2.5
Ca/Cr, mg/mg	0.17 ± 0.05	0.19 ± 0.08	0.19 ± 0.10	0.18 ± 0.07

Cr, creatinine; FE_{Na}, FE_K, FE_{Cl}, and FE_{Mg} represent the fractional excretion of Na$^+$, K$^+$, Cl$^-$, and Mg^{2+}, respectively.
*$P < 0.05$ vs. WT on the same diet.

Table 2. BP and blood and urine biochemistry values in KSP-OSR1$^{-/-}$ mice

Diet	Normal		Low Na$^+$	
Genotype (*n*)	WT (*n* = 10)	KSP-OSR$^{-/-}$ (*n* = 10)	WT (*n* = 8)	KSP-OSR$^{-/-}$ (*n* = 8)
BP, mmHg				
Systolic	110 ± 3	107 ± 4	109 ± 2	101 ± 6*
Diastolic	57 ± 4	60 ± 7	51 ± 4	46 ± 9
Mean	75 ± 2.3	74 ± 6	69 ± 3	62 ± 7
Weight, g	23.6 ± 3.5	22.8 ± 4.3	22.1 ± 4.5	23.2 ± 5.3
Plasma				
PAC, pg/mL	999 ± 329	867 ± 216	1,433 ± 265	1,289 ± 332
PRA, ng·mL·h	8.7 ± 3.5	7.9 ± 4.2	11.4 ± 3.5	12.3 ± 4.2
Na$^+$, mmol/L	154 ± 3	153 ± 2	152 ± 6	150 ± 5
K$^+$, mmol/L	4.2 ± 0.2	3.7 ± 0.2*	4.3 ± 0.3	3.6 ± 0.3*
Cl$^-$, mmol/L	114 ± 3	112 ± 4	114 ± 3	112 ± 4
Ca^{2+}, mg/dL	9.8 ± 0.3	9.7 ± 0.2	9.8 ± 0.3	9.7 ± 0.2
Mg^{2+}, mg/dL	2.9 ± 0.2	3.0 ± 0.1	2.8 ± 0.3	3.0 ± 0.3
Cr, mg/dL	0.14 ± 0.06	0.13 ± 0.05	0.13 ± 0.05	0.12 ± 0.08
Urine, mL/d	1.92 ± 0.80	2.68 ± 0.21*	1.54 ± 0.80	2.13 ± 0.68*
Na$^+$, μmol/d	232 ± 72	250 ± 55	93 ± 17	103 ± 26
K$^+$, μmol/d	311 ± 122	375 ± 110	489 ± 222	518 ± 110
Cl$^-$, μmol/d	203 ± 84	247 ± 78	65 ± 34	72 ± 24
Mg^{2+}, mg/d	0.60 ± 0.29	0.56 ± 0.14	0.58 ± 0.21	0.55 ± 0.15
FE_{Na}, %	0.55 ± 0.14	0.58 ± 0.27	0.22 ± 0.06	0.24 ± 0.12
FE_K, %	20.1 ± 4.1	29.5 ± 4.5*	22.1 ± 6.2	32.8 ± 6.5*
FE_{Cl}, %	0.52 ± 0.14	0.54 ± 0.16	0.20 ± 0.04	0.22 ± 0.05
FE_{Mg}, %	11.4 ± 2.1	10.1 ± 1.1	10.4 ± 3.1	9.1 ± 2.5
Ca/Cr, mg/mg	0.16 ± 0.03	0.21 ± 0.04*	0.18 ± 0.02	0.23 ± 0.05*

Cr, creatinine; FE_{Na}, FE_K, FE_{Cl}, and FE_{Mg} represent the fractional excretion of Na$^+$, K$^+$, Cl$^-$, and Mg^{2+}, respectively.
*$P < 0.05$ vs. WT on the same diet

electrolyte abnormalities (Table 1). The KSP-OSR1$^{-/-}$ mice had normal BP; however, unlike the global OSR1$^{+/-}$ mice, they showed significant hypokalemia with an increased fractional excretion of K$^+$ (FE_K) ($P < 0.05$) and hypercalciuria ($P < 0.05$) (Table 2). In addition, the ambient osmolarity of spot urine was significantly reduced in KSP-OSR1$^{-/-}$ mice (1,805 ± 389 vs. 2,414 ± 525 mOsm/L in WT, $n = 10$; $P < 0.05$). When the global OSR1$^{+/-}$ and KSP-OSR1$^{-/-}$ mice were fed a low-Na$^+$ diet (0.05% Na$^+$ wt/wt), the

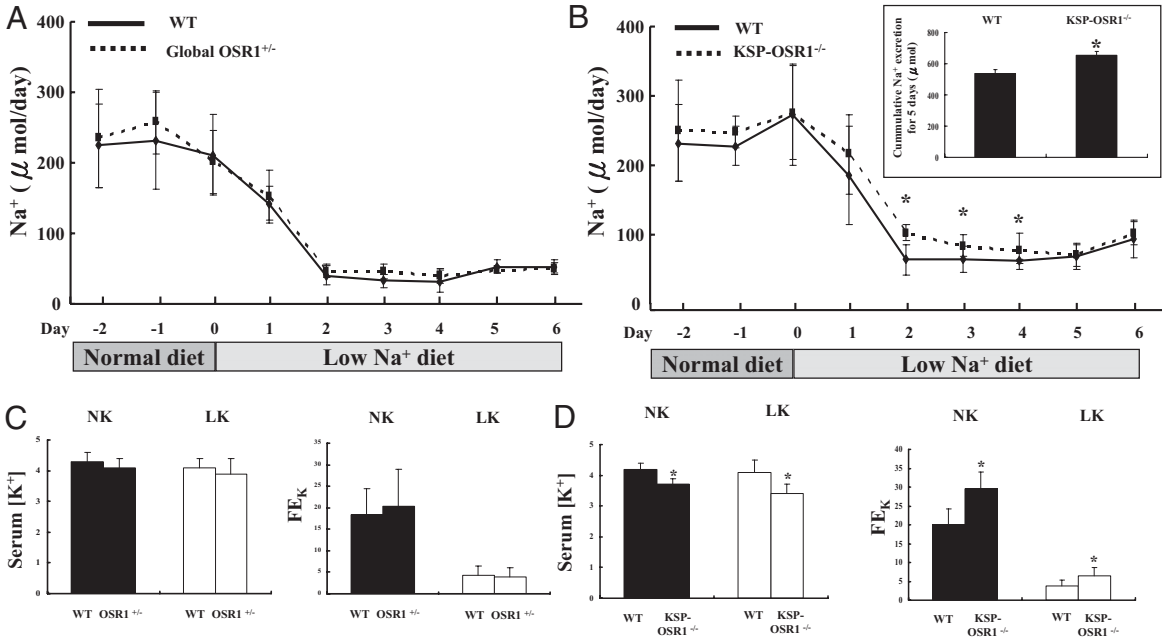

Fig. 1. Na$^+$ balance and renal K$^+$ handling in OSR1$^{+/-}$ and KSP-OSR1$^{-/-}$ mice. The daily urine Na$^+$ excretion rate in WT and global OSR1$^{+/-}$ (*A*) or KSP-OSR1$^{-/-}$ (*B*) mice on a normal-Na$^+$ diet for 3 d and then on a low-Na$^+$ diet for 6 d was determined. (*B*, *Inset*) Cumulative Na$^+$ excretion from day 1 to day 5 of the low-Na$^+$ diet between WT and KSP-OSR1$^{-/-}$ mice. *$P < 0.05$ vs. WT ($n = 6$ per group). Serum K$^+$ concentration and urinary FE_K in WT, OSR1$^{+/-}$ (*C*), and KSP-OSR1$^{-/-}$ (*D*) mice on a normal-K$^+$ (NK) diet and a low-K$^+$ (LK) diet. *$P < 0.05$ vs. WT ($n = 8$ per group).

PHYSIOLOGY

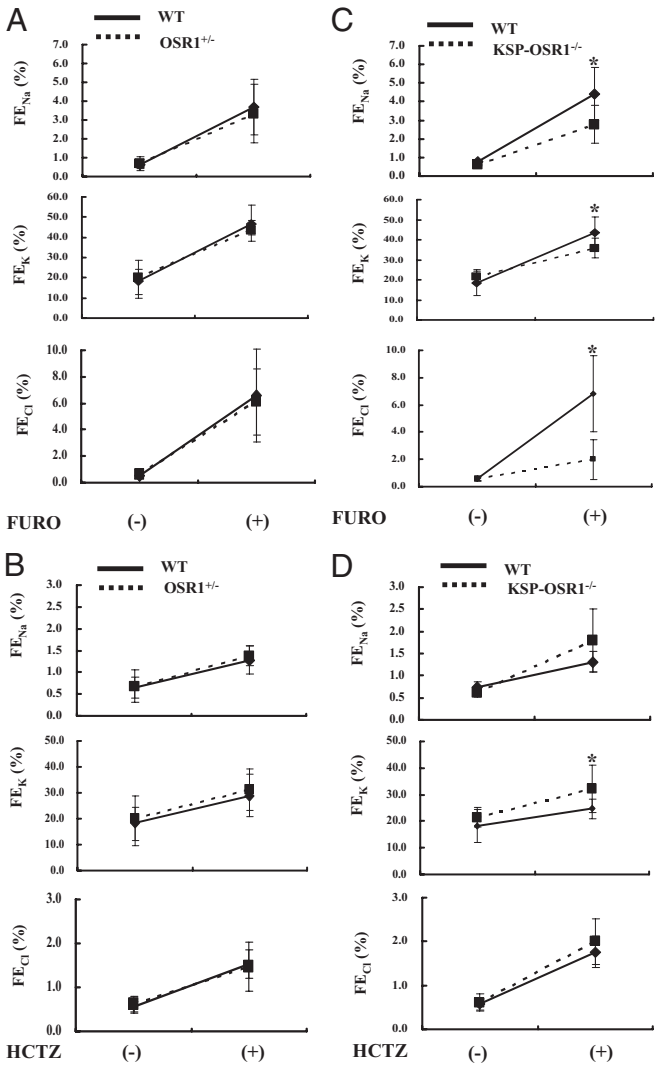

Fig. 2. Effect of furosemide (FURO) and HCTZ administration on Na^+, K^+, and Cl^- excretion. FE_{Na}, FE_K, and FE_{Cl} represent the fractional excretion of Na^+, K^+, and Cl^-, respectively. Preserved response of FE_{Na}, FE_K, and FE_{Cl} in OSR1$^{+/-}$ mice after FURO (*A*) and HCTZ (*B*) treatment is shown. *$P < 0.05$ vs. WT ($n = 6$ per group). There was a blunted response of FE_{Na}, FE_K, and FE_{Cl} in KSP-OSR1$^{-/-}$ mice after FURO treatment (*C*) but a similar response of FE_{Na}, FE_K, and FE_{Cl} between WT and KSP-OSR1$^{-/-}$ mice after HCTZ (*D*) treatment. *$P < 0.05$ vs. WT ($n = 6$ per group).

severity of hypotension did not increase in OSR1$^{+/-}$ mice, whereas the previously normotensive KSP-OSR1$^{-/-}$ mice developed relative systolic hypotension ($P < 0.05$ for systolic BP only). A low-Na^+ diet also caused significant increases in the plasma aldosterone concentration (PAC) and plasma renin activity (PRA) in both global OSR1$^{+/-}$ and KSP-OSR1$^{-/-}$ mice, which were not significantly different from their WT littermates (Tables 1 and 2).

Renal Na^+ and K^+ Handling in Global OSR1$^{+/-}$ and KSP-OSR1$^{-/-}$ Mice. We further evaluated renal Na^+ and K^+ handling in the global OSR1$^{+/-}$ and KSP-OSR1$^{-/-}$ mice. On normal Na^+ diets, all these different groups of mice had similar urine Na^+ excretion rates and fractional excretion of Na^+ (FE_{Na}) (Tables 1 and 2). On paired-fed low-Na^+ diets, the urinary Na^+ excretion quickly dropped in all three groups (WT, global OSR1$^{+/-}$, and KSP-OSR1$^{-/-}$) of mice. There was no significant difference in the degree of reduced urine Na^+ excretion between the global OSR1$^{+/-}$ and WT littermates (Fig. 1*A*). However, KSP-OSR1$^{-/-}$ mice clearly demonstrated more urine Na^+ excretion than WT controls on the second, third, and fourth days (Fig. 1*B*), supporting the presence of a renal tubular defect in KSP-OSR1$^{-/-}$ mice. Compared with WT controls, the average increased Na^+ excretion was 115 ± 7 μmol per mouse for the 6 d of the low-Na^+ diet in the KSP-OSR1$^{-/-}$ mice (Fig. 1*B*).

We then evaluated K^+ handling in the mice on a low-K^+ diet (0.3% K^+ wt/wt) for 6 d. WT and OSR1$^{+/-}$ mice showed no significant difference in serum K^+ concentration [3.9 ± 0.5 mmol/L in OSR1$^{+/-}$ ($n = 8$) vs. 4.1 ± 0.3 mmol/L in WT ($n = 8$); $P = 0.48$] and urinary FE_K [$4.0 \pm 2.1\%$ in OSR1$^{+/-}$ ($n = 8$) vs. $4.3 \pm 2.1\%$ in WT ($n = 8$); $P = 0.61$] (Fig. 1*C*). The KSP-OSR1$^{-/-}$ mice, which already had hypokalemia on a regular diet, showed more pronounced hypokalemia [3.5 ± 0.3 mmol/L in KSP-OSR1$^{-/-}$ ($n = 8$) vs. 4.1 ± 0.4 mmol/L in WT ($n = 8$); $P < 0.05$] and urinary FE_K [$6.5 \pm 2.2\%$ in KSP-OSR1$^{-/-}$ ($n = 8$) vs. $3.8 \pm 1.5\%$ in WT ($n = 8$); $P < 0.05$] (Fig. 1*D*) after a low-K^+ diet.

Diuretic Response in Global OSR1$^{+/-}$ and KSP-OSR1$^{-/-}$ Mice. To determine the function of NKCC2 and NCC, two substrates of OSR1, in these global OSR1$^{+/-}$ and KSP-OSR1$^{-/-}$ mice, we administered the NKCC2 inhibitor furosemide and NCC inhibitor hydrochlorothiazide (HCTZ), respectively. Like WT mice, global OSR1$^{+/-}$ mice showed a dramatic and similar increase in the FE_{Na}, FE_K, and FE_{Cl} in response to furosemide (Fig. 2*A*) and HCTZ (Fig. 2*B*), suggesting that their NKCC2 and NCC functions were not obviously affected. Compared with WT and global OSR1$^{+/-}$ mice, KSP-OSR1$^{-/-}$ mice exhibited a blunted response to furosemide (Fig. 2*C*) but a normal response to HCTZ (Fig. 2*D*), indicating that their NKCC2 function was reduced and NCC function was well preserved (Fig. 2*D*).

Expression of OSR1, SPAK, and NKCC1 in Aortic Tissues of Global OSR1$^{+/-}$ Mice. Because OSR1, SPAK, and NKCC1 are coexpressed in vascular smooth muscle and NKCC1 activity is known to play an important role in the regulation of aortic contractility and BP (1, 2), we examined whether the OSR1/SPAK-NKCC1 pathway could be involved in the hypotension of global OSR1$^{+/-}$ mice. Relative protein expression of total OSR1 ($59 \pm 22\%$; $P < 0.01$), p-OSR1 ($44 \pm 12\%$; $P < 0.01$), and p-SPAK ($54.6 \pm 2.6\%$; $P < 0.01$) was significantly reduced, along with dramatically reduced p-NKCC1 expression (T206) ($53 \pm 22\%$; $P < 0.01$) despite unchanged total SPAK and NKCC1 abundance in aortic tissue (Fig. 3). These findings suggested that defective phosphorylation of OSR1 may cause decreased NKCC1 phosphorylation in blood vessels, which led to the lower BP.

Renal OSR1, SPAK, NKCC2, and NCC in Global OSR1$^{+/-}$ and KSP-OSR1$^{-/-}$ Mice. In the kidneys, we had previously reported that OSR1 is mainly distributed in the TAL to downstream renal tubules and is dominantly expressed in the medulla, colocalizing with NKCC2 (19). Because KSP-OSR1$^{-/-}$ mice displayed a BS-like phenotype with hypercalciuria and normal magnesemia and a blunted response to furosemide corresponding to a TAL lesion rather than GS physiology (a DCT lesion with hypocalciuria and hypomagnesemia) (20), the expression of total and p-OSR1, SPAK, NKCC2, and NCC in the kidney of both OSR1$^{+/-}$ and KSP-OSR1$^{-/-}$ mice was further evaluated by semiquantitative immunoblotting (IB).

Although renal total OSR1 ($75 \pm 11\%$; $P < 0.05$) and p-OSR1 ($69 \pm 21\%$; $P < 0.05$) expression was reduced in OSR1$^{+/-}$ mice (Fig. 4*A*), p-SPAK ($128 \pm 11\%$; $P < 0.05$) was mildly increased (Fig. 4*B*). The expression of total NKCC2 was not affected, but p-NKCC2 (T96) ($72 \pm 15\%$; $P < 0.05$) was significantly reduced (Fig. 4*C*). Total NCC ($135 \pm 7\%$; $P < 0.05$), p-NCC (T58) $121 \pm 6\%$; $P < 0.05$), and p-NCC (S71) ($156 \pm 8\%$; $P < 0.05$) were also significantly increased (Fig. 4*D* and Fig. S3*A*). As expected, total OSR1 and p-OSR1 were virtually absent from the kidney tissue of KSP-OSR1$^{-/-}$ mice (Fig. 5*A*). However, total SPAK ($130 \pm 13\%$; $P < 0.05$) and p-SPAK ($138 \pm 13\%$; $P < 0.05$) (Fig. 5*B*) were markedly increased. As in OSR1$^{+/-}$ mice, expression of total NKCC2 was not affected but p-NKCC2 (T96) was more dramatically reduced ($32 \pm 14\%$; $P < 0.01$) (Fig. 5*C*). Total NCC ($158 \pm 9\%$; $P < 0.01$),

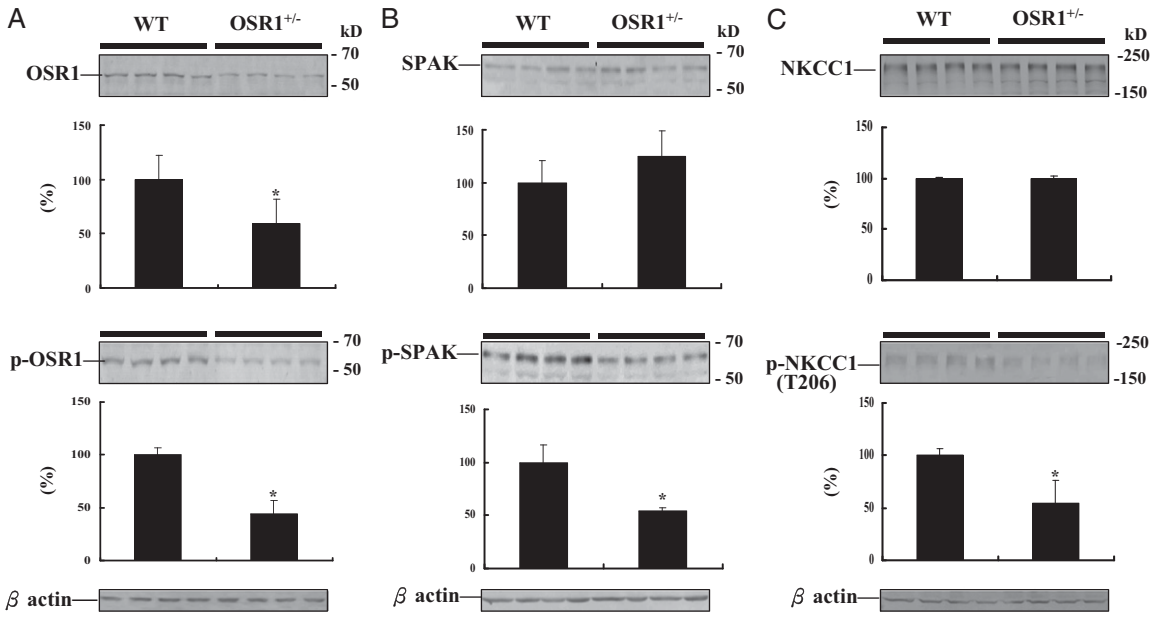

Fig. 3. Expression of OSR1, SPAK, and NKCC1 in aortic tissues of OSR1$^{+/-}$ mice. Semiquantitative IB (*Upper*) and densitometry (*Lower*) of total and p-OSR1 (*A*), total and p-SPAK (*B*), and total and p-NKCC1 (T206) (*C*) in aortic tissues of WT and OSR1$^{+/-}$ mice (n = 4 per group). *P < 0.05 vs. WT.

p-NCC (T53) (138 ± 11%; $P < 0.05$), p-NCC (T58) (127 ± 9%; $P < 0.05$), and p-NCC (S71) (145 ± 15%; $P < 0.05$) (Fig. 5*D* and Fig. S3*B*) were significantly increased in KSP-OSR1$^{-/-}$ mice.

We also examined the cellular localization of NKCC2 and NCC in the kidney tissue of OSR1$^{+/-}$ and KSP-OSR1$^{-/-}$ mice. The cellular distribution of total NKCC2 and p-NKCC2 (T96) was still luminally condensed, albeit less so for p-NKCC2 (T96) (Fig. S4 *A* and *B*). Likewise, total NCC and p-NCC were still luminally condensed (Fig. S4 *C* and *D*).

Discussion

In this study, we generated and analyzed global and KSP-OSR1 KO mice to elucidate the physiological role of OSR1 in vivo in the regulation of the NKCC1 and kidney-specific NKCC2 and NCC, focusing on BP and renal tubular Na^+ reabsorption. As previously reported in OSR1 gene-trapped or kinase-dead knock-in mice (21, 22), global homozygous OSR1$^{-/-}$ mice were embryonically lethal. Heterozygous OSR1$^{+/-}$ mice exhibited hypotension, markedly reduced p-NKCC1 abundance in aortic tissue, and attenuated p-NKCC2 in kidney. KSP-OSR1$^{-/-}$ mice recapitulated the reduced renal Na^+ reabsorption on low-Na^+ diets and remarkably decreased expression of p-NKCC2. They also had a blunted response to furosemide and a parallel increase in NCC expression and phosphorylation, supporting the notion that TAL function was defective. These results indicate that OSR1 is crucial not only in the regulation of BP but in renal tubular Na^+ reabsorption, primarily in the TAL rather than the DCT.

In the global OSR1$^{+/-}$ mice, markedly decreased p-NKCC1 in aortic tissue and kidneys may contribute to obvious hypotension. NKCC1, as a downstream target of OSR1, has been known to play a pivotal role in BP control through vascular and renal effects, as shown in NKCC1 KO mice (1–4). On the one hand, inactivation of NKCC1 in blood vessels causes reduced intracellular Cl^- concentration and, consequently, decreased Ca^{2+} influx through L-type Ca^{2+} channels, which may lead to vessel relaxation and hypotension (23). On the other hand, defective NKCC1 expression in the basolateral membrane of inner medullary collecting ducts and renin-producing juxtaglomerular (JG) cells (24) may cause the impairment of renal Na^+ reabsorption. However, hyperreninemia and hyperaldosteronism with increased renal Na^+ transporters, including NKCC2 and NCC observed in NKCC1 KO mice, could help minimize hypotension (3, 4).

Reminiscent of the reduced NKCC1 phosphorylation with reduced aortic contractility in SPAK$^{+/-}$ mice featuring hypotension but normal serum and urine electrolytes (19), the hypotension observed in global OSR1$^{+/-}$ mice reiterates the importance of OSR1/SPAK-NKCC1 phosphorylation signaling in the vascular tissue on BP control. Because both OSR1$^{+/-}$ and SPAK$^{+/-}$ mice had normal total NKCC1 but reduced p-NKCC1, it appeared that intact expression of both OSR1 and SPAK was required for adequate NKCC1 phosphorylation in the aortic tissue. Based on the attenuated rather than increased p-SPAK expression in the aortic tissue of OSR1$^{+/-}$ mice, SPAK phosphorylation may be dependent on the OSR1 activity in the vessels.

In addition to vascular NKCC1, kidney-specific NKCC2 and NCC, two other OSR1 substrates in the TAL and DCT, respectively (5), were also examined in global OSR1$^{+/-}$ mice. A significant decrease in p-NKCC2 and a parallel increase in both p-SPAK and p-NCC in the OSR1$^{+/-}$ mice strongly suggested that a salt-wasting phenotype was present. Based on the Guyton type renal function curve (a plot between mean arterial pressure and urinary Na^+ intake and excretion) (25), OSR1$^{+/-}$ mice showed a shift to the left, supporting a defect in renal Na^+ transport. Their renal tubule Na^+ defect was mild, however, because they did not exhibit negative renal Na^+ balance even on low-salt diets. Furthermore, their responses to furosemide and thiazide challenges were also normal. Nevertheless, hypotension in OSR1$^{+/-}$ mice might help dampen the tendency of impaired renal Na^+ reabsorption. In response to vascular hypotension or renal Na^+ wasting, one should expect an increase in PRA and PAC. However, PRA and PAC were similar between the WT and OSR1$^{+/-}$ mice, suggesting that PRA and PAC were inappropriately low in OSR1$^{+/-}$ mice. Perhaps the reduced p-NKCC2 observed in OSR1$^{+/-}$ mice may have blunted tubuloglomerular feedback, leading to the impaired release of renin from JG cells as shown in NKCC2 isoform KO mice (26, 27). However, we could not exclude the direct regulation of aldosterone secretion by OSR1, which was also abundantly expressed in adrenal tissues.

To focus on the specific role of OSR1 in the regulation of NKCC2 and NCC in the kidney, we further created the KSP-OSR1 KO mice. NKCC2 has three different full-length splice variants called A, B, and F isoforms (5). Inactivating mutations in NKCC2 can cause antenatal BS, an autosomal recessive renal Na^+-losing nephropathy with chronic hypokalemia and hypercalciuria with

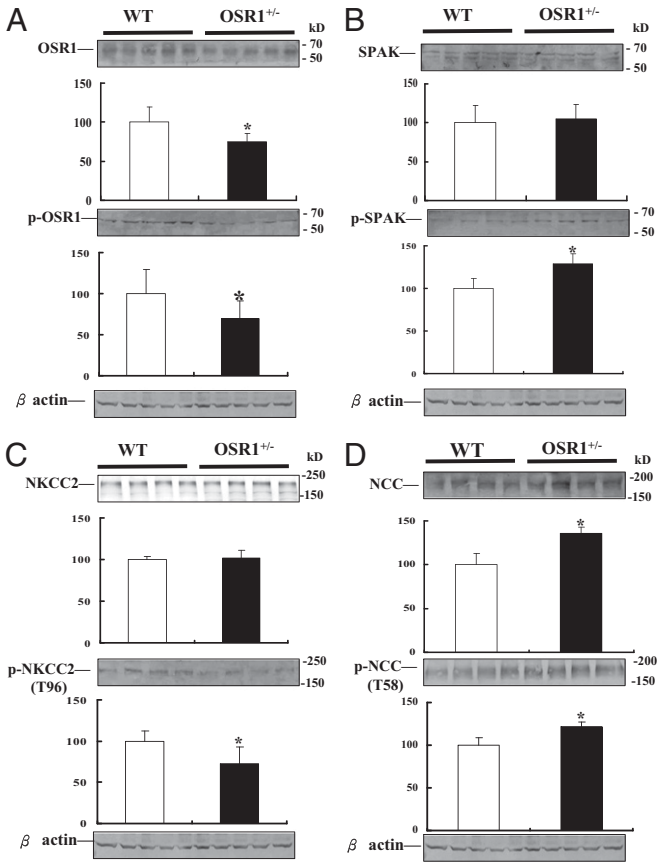

Fig. 4. Expression of OSR1, SPAK, NKCC2, and NCC in kidney tissues of OSR1$^{+/-}$ mice. Semiquantitative IB (*Upper*) and densitometry (*Lower*) of total and p-OSR1 (*A*), total and p-SPAK (*B*), total and p-NKCC2 (T96) (*C*), and total and p-NCC (T58) (*D*) in kidney tissues of WT and OSR1$^{+/-}$ mice (n = 4 per group). *P < 0.05 vs. WT.

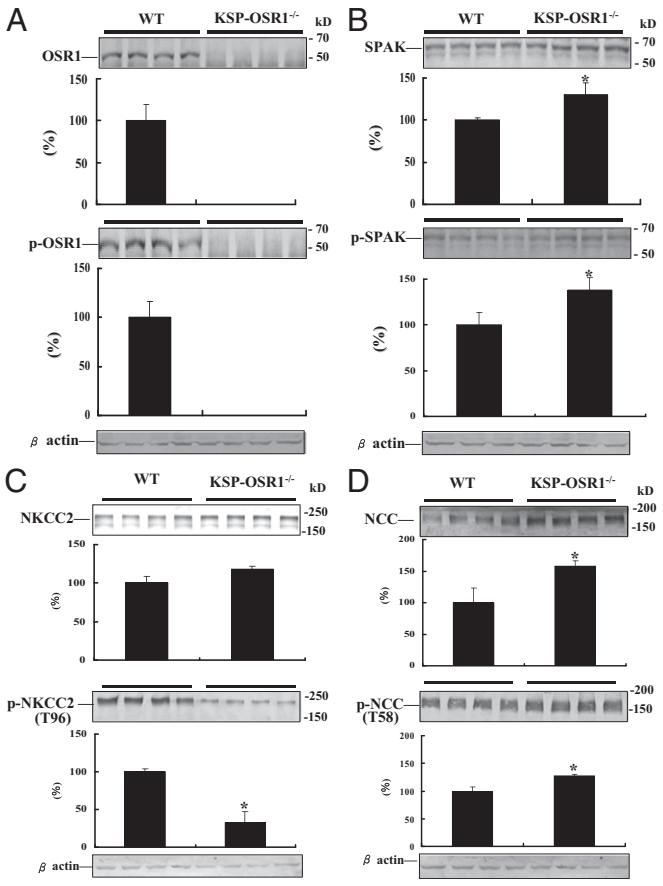

Fig. 5. Expression of OSR1, SPAK, NKCC2, and NCC in kidney tissues of KSP-OSR1$^{-/-}$ mice. Semiquantitative IB (*Upper*) and densitometry (*Lower*) of total and p-OSR1 (*A*), total and p-SPAK (*B*), total and p-NKCC2(T96) (*C*), and total and p-NCC (T58) (*D*) in kidney tissues of WT and KSP-OSR1$^{-/-}$ mice (n = 4 per group). *P < 0.05 vs. WT.

nephrocalcinosis (9). Growth retardation and impaired urine concentration with polyuria are also prominent features in patients who have BS with NKCC2 mutations (28, 29) and in total NKCC2-null mice (30). Unlike total NKCC2-null mice, NKCC2 A- or B-isoform null mice exhibit normal growth but a mild defect in the TAL, with slightly reduced urine osmolality and no polyuria (26, 27). Our KSP-OSR1$^{-/-}$ mice had marked diminution in p-NKCC2 expression and a partially blunted response to furosemide, indicating a moderate defective function of the TAL. Because mice have very high Na^+ intake, a defect in renal tubular Na^+ absorption can be concealed without modification of dietary Na^+. On a low-Na^+ diet, KSP-OSR1$^{-/-}$ mice showed more urine Na^+ excretion than WT mice, supporting the presence of a renal tubular defect. The salt phenotype in KSP-OSR1$^{-/-}$ mice resembled that in NKCC2 A or B KO mice because they all had residual NKCC2 function. Furthermore, the enhanced total and p-SPAK and total p-NCC expression seen in these mice may be compensatory responses to the Na^+ reabsorption defect upstream.

In the kidneys, we have reported that OSR1 and SPAK are expressed in both TAL and DCT. On the one hand, SPAK is mainly expressed in the cortex, especially in the DCT, and SPAK$^{-/-}$ mice with reduced total and p-NCC expression manifest a GS-like syndrome. On the other hand, OSR1 is predominantly expressed in the medulla, especially in the TAL (19). It is reasonable to expect that NKCC2 but not NCC might be the major substrate of OSR1 in renal tubules. Consistent with this notion, we observed reduced p-NKCC2 but increased total and p-NCC abundance in KSP-OSR1$^{-/-}$ mice. However, unlike the decreased NCC phosphorylation in the setting of decreased total NCC abundance in SPAK$^{-/-}$ mice (19), the reduced NKCC2 phosphorylation with unchanged total NKCC2 abundance in KSP-OSR1$^{-/-}$ mice suggests a different mechanism at work. A recent elegant study has shown that adaptor protein (AP)-3, a lysosomal protein, is involved in the sorting process of NCC from the trans-Golgi network to lysosomes and from endosomes to lysosomes (31). Of interest, the most important SPAK/OSR1 phosphoacceptor site on NCC, the T58 residue in the N terminus, is embedded in one of the putative canonical AP-3 binding motifs (YXXθ) and participates in the sorting mechanism of NCC. However, none of the putative canonical AP-3 binding motifs are found in the NKCC2 N terminus. Furthermore, NKCC2 phosphorylation at S130, another important phosphoacceptor, has been shown to be activated by SPAK/OSR1-independent pathways, perhaps via AMP-activated protein kinase, and may also be involved in the regulation of NKCC2 apical sorting (32). KSP-OSR1$^{-/-}$ and SPAK$^{-/-}$ mice may be used further to explore the mechanisms of NKCC2 and NCC phosphorylation on their protein trafficking.

In addition to Na^+ wasting, KSP-OSR1$^{-/-}$ mice had other electrolyte disturbances, such as hypercalciuria and hypokalemia with renal K^+ wasting. The TAL also accounts for 20–25% of filtrated K^+ and Ca^{2+} reabsorption in parallel with Na^+ reabsorption. Although K^+ is directly reabsorbed by NKCC2, the reabsorption of Na^+ provides the main driving force for Ca^{2+} reabsorption via paracellular routes (5). Reduced NKCC2 function would thus impede normal K^+ and Ca^{2+} reabsorption in the TAL, leading to increased urine K^+ and Ca^{2+} excretion. When these

mice were fed low-K^+ diets, significant hypokalemia was maintained, supporting that KSP-OSR1$^{-/-}$ mice had renal K^+ wasting.

In conclusion, the analysis of global OSR1$^{+/-}$ and KSP-OSR1$^{-/-}$ mice sheds some light on the physiological role of OSR1 in BP regulation and renal Na^+ handling. OSR1$^{+/-}$ mice exhibit hypotension associated with the reduced p-SPAK and p-NKCC1 abundance in aortic tissue and decreased p-NKCC2 with an increase in both p-SPAK and p-NCC in the kidney, which is indicative of a salt-wasting phenotype. KSP-OSR1$^{-/-}$ mice show markedly decreased p-NKCC2 expression in the TAL with a blunted response to furosemide and enhanced p-NCC expression in the DCT, supporting the notion that NKCC2 is the main target of OSR1 and accounts for the BS-like phenotype. These results show that OSR1 plays a dual role in arterial tonicity and renal Na^+ reabsorption, primarily through NKCC1 and NKCC2, respectively. The development of OSR1 inhibitors suppressing vascular NKCC1 and renal NKCC2 may be a promising direction for antihypertensive therapy in the future.

Materials and Methods

Blood and Urine Analysis and BP Measurement. The phenotype of male mice was evaluated at the age of 12–14 wk. Mice were kept in metabolic cages for 24-h urine collection. Urine osmolarities under ambient conditions were determined using spot urine samples. Blood pressure, plasma and urine electrolytes, and hormone were obtained and measured as previously described (17, 33).

Na^+ and K^+ Balance Study. The mice were raised on a 12-h day/night cycle, fed a normal rodent chow diet, and given plain drinking water ad libitum. For the evaluation of renal Na^+ and K^+ handing, a low-Na^+ diet or low-K^+ diet was fed for 6 d (34).

HCTZ and Furosemide Challenge Studies. HCTZ (12.5 mg/kg) and furosemide (15 mg/kg) were administered i.p., respectively, to the mice (19). Urine samples in the 4 h after a single-dose treatment were collected for analysis.

IB and Immunofluorescence Stain. Semiquantitative IB and immunofluorescence (IF) microscopy was carried out as previously described (17, 33). In addition to our previously generated rabbit anti–p-NCC (T53, T58, and S71) (17, 35), an antibody that could recognize both p-OSR1(S325) and p-SPAK(S383) simultaneously (14, 18), and rabbit anti–p-NKCC2 (T96), which could also recognize p-NKCC1(T206) (19), other commercially available primary antibodies used included rabbit anti-SPAK (Cell Signaling) (14, 18, 36), NKCC2 (Alpha Diagnostic) (19), NCC (Millipore) (17), mouse anti-OSR1 (Abnova) (14, 18), and NKCC (T4) (37). Alkaline phosphatase-conjugated anti-IgG antibodies (Promega) were used as secondary antibodies for IB, and Alexa 488 or 546 dye-labeled (Molecular Probes) secondary antibodies were used for IF microscopy. IF images were obtained using a LSM510 confocal microscope (Carl Zeiss).

Statistical Analysis. All results are expressed as mean ± SD. Results obtained for the OSR1$^{+/-}$ or KSP-OSR1$^{-/-}$ mice were compared with those from their WT littermates by means of the Student *t* test or, if the data violated a normal distribution, the nonparametric Mann–Whitney test. A *P* value less than 0.05 was considered to be statistically significant.

ACKNOWLEDGMENTS. We thank the Transgenic Mouse Model Core Facility of the National Research Program for Genomic Medicine, (NRPGM) and the National Core Facility Program for Biotechnology (NCFPB), National Science Council, Taiwan, for the provision of technical services. We also thank Yin Sun and Tai-Hsiang Chang for mice genotyping and preparation of tissue samples for IB and IF staining. This study was supported, in part, by the National Science Council, Taiwan (Grants NSC 100-2314-B-016-018-MY3 and NSC-98-2314-B-016-002-MY3), the Research Fund of Tri-Service General Hospital (Grant TSGH-C-100-040), and Japan-Taiwan Joint Research Program, Interchange Association, Japan.

1. Meyer JW, et al. (2002) Decreased blood pressure and vascular smooth muscle tone in mice lacking basolateral Na(+)-K(+)-2Cl(-) cotransporter. *Am J Physiol Heart Circ Physiol* 283:H1846–H1855.
2. Garg P, et al. (2007) Effect of the Na-K-2Cl cotransporter NKCC1 on systemic blood pressure and smooth muscle tone. *Am J Physiol Heart Circ Physiol* 292:H2100–H2105.
3. Wall SM, et al. (2006) Hypotension in NKCC1 null mice: Role of the kidneys. *Am J Physiol Renal Physiol* 290:F409–F416.
4. Kim SM, et al. (2008) Salt sensitivity of blood pressure in NKCC1-deficient mice. *Am J Physiol Renal Physiol* 295:F1230–F1238.
5. Gamba G (2005) Molecular physiology and pathophysiology of electroneutral cation-chloride cotransporters. *Physiol Rev* 85:423–493.
6. Orlov SN, Adragna NC, Adarichev VA, Hamet P (1999) Genetic and biochemical determinants of abnormal monovalent ion transport in primary hypertension. *Am J Physiol* 276:C511–C536.
7. Orlov SN, Tremblay J, Hamet P (2010) NKCC1 and hypertension: A novel therapeutic target involved in the regulation of vascular tone and renal function. *Curr Opin Nephrol Hypertens* 19:163–168.
8. Wilson FH, et al. (2001) Human hypertension caused by mutations in WNK kinases. *Science* 293:1107–1112.
9. Simon DB, et al. (1996) Bartter's syndrome, hypokalaemic alkalosis with hypercalciuria, is caused by mutations in the Na-K-2Cl cotransporter NKCC2. *Nat Genet* 13:183–188.
10. Simon DB, et al. (1996) Gitelman's variant of Bartter's syndrome, inherited hypokalaemic alkalosis, is caused by mutations in the thiazide-sensitive Na-Cl cotransporter. *Nat Genet* 12:24–30.
11. Tamari M, Daigo Y, Nakamura Y (1999) Isolation and characterization of a novel serine threonine kinase gene on chromosome 3p2. 3. *J Hum Genet* 44:2–116–21120.
12. Johnston AM, et al. (2000) SPAK, a STE20/SPS1-related kinase that activates the p38 pathway. *Oncogene* 19:4290–4297.
13. Piechotta K, Lu J, Delpire E (2002) Cation chloride cotransporters interact with the stress-related kinases Ste20-related proline-alanine-rich kinase (SPAK) and oxidative stress response 1 (OSR1). *J Biol Chem* 277:50812–50819.
14. Moriguchi T, et al. (2005) WNK1 regulates phosphorylation of cation-chloride-coupled cotransporters via the STE20-related kinases, SPAK and OSR1. *J Biol Chem* 280: 42685–42693.
15. Vitari AC, Deak M, Morrice NA, Alessi DR (2005) The WNK1 and WNK4 protein kinases that are mutated in Gordon's hypertension syndrome phosphorylate and activate SPAK and OSR1 protein kinases. *Biochem J* 391:17–24.
16. Huang CL, Yang SS, Lin SH (2008) Mechanism of regulation of renal ion transport by WNK kinases. *Curr Opin Nephrol Hypertens* 17:519–525.
17. Yang SS, et al. (2007) Molecular pathogenesis of pseudohypoaldosteronism type II: Generation and analysis of a Wnk4(D561A/+) knockin mouse model. *Cell Metab* 5: 331–344.
18. Ohta A, et al. (2009) Targeted disruption of the Wnk4 gene decreases phosphorylation of Na-Cl cotransporter, increases Na excretion and lowers blood pressure. *Hum Mol Genet* 18:3978–3986.
19. Yang SS, et al. (2010) SPAK-knockout mice manifest Gitelman syndrome and impaired vasoconstriction. *J Am Soc Nephrol* 21:1868–1877.
20. Cheng CJ, Shiang JC, Hsu YJ, Yang SS, Lin SH (2007) Hypocalciuria in patients with Gitelman syndrome: Role of blood volume. *Am J Kidney Dis* 49:693–700.
21. Delpire E, Gagnon KB (2008) SPAK and OSR1: STE20 kinases involved in the regulation of ion homoeostasis and volume control in mammalian cells. *Biochem J* 409:321–331.
22. Rafiqi FH, et al. (2010) Role of the WNK-activated SPAK kinase in regulating blood pressure. *EMBO Mol Med* 2:63–75.
23. Orlov SN, Mongin AA (2007) Salt-sensing mechanisms in blood pressure regulation and hypertension. *Am J Physiol Heart Circ Physiol* 293:H2039–H2053.
24. Kaplan MR, Plotkin MD, Brown D, Hebert SC, Delpire E (1996) Expression of the mouse Na-K-2Cl cotransporter, mBSC2, in the terminal inner medullary collecting duct, the glomerular and extraglomerular mesangium, and the glomerular afferent arteriole. *J Clin Invest* 98:723–730.
25. Guyton AC (1989) Roles of the kidneys and fluid volumes in arterial pressure regulation and hypertension. *Chin J Physiol* 32:49–57.
26. Oppermann M, et al. (2006) Macula densa control of renin secretion and preglomerular resistance in mice with selective deletion of the B isoform of the Na,K,2Cl co-transporter. *J Am Soc Nephrol* 17:2143–2152.
27. Oppermann M, et al. (2007) Renal function in mice with targeted disruption of the A isoform of the Na-K-2Cl co-transporter. *J Am Soc Nephrol* 18:440–448.
28. Bartter FC, Pronove P, Gill JR, Jr., MacCardle RC (1962) Hyperplasia of the juxtaglomerular complex with hyperaldosteronism and hypokalemic alkalosis. A new syndrome. *Am J Med* 33:811–828.
29. Kurtz I (1998) Molecular pathogenesis of Bartter's and Gitelman's syndromes. *Kidney Int* 54:1396–1410.
30. Takahashi N, et al. (2000) Uncompensated polyuria in a mouse model of Bartter's syndrome. *Proc Natl Acad Sci USA* 97:5434–5439.
31. Subramanya AR, Liu J, Ellison DH, Wade JB, Welling PA (2009) WNK4 diverts the thiazide-sensitive NaCl cotransporter to the lysosome and stimulates AP-3 interaction. *J Biol Chem* 284:18471–18480.
32. Richardson C, et al. (2011) Regulation of the NKCC2 ion cotransporter by SPAK-OSR1-dependent and -independent pathways. *J Cell Sci* 124:789–800.
33. Yang SS, et al. (2010) Generation and analysis of the thiazide-sensitive Na+ -Cl- cotransporter (Ncc/Slc12a3) Ser707X knockin mouse as a model of Gitelman syndrome. *Hum Mutat* 31:1304–1315.
34. Liu Z, et al. (2011) Downregulation of NCC and NKCC2 cotransporters by kidney-specific WNK1 revealed by gene disruption and transgenic mouse models. *Hum Mol Genet* 20:855–866.
35. Chiga M, et al. (2008) Dietary salt regulates the phosphorylation of OSR1/SPAK kinases and the sodium chloride cotransporter through aldosterone. *Kidney Int* 74:1403–1409.
36. Wang Y, et al. (2009) From the Cover: Whole-genome association study identifies STK39 as a hypertension susceptibility gene. *Proc Natl Acad Sci USA* 106:226–231.
37. Lytle C, Xu JC, Biemesderfer D, Forbush B, 3rd (1995) Distribution and diversity of Na-K-Cl cotransport proteins: A study with monoclonal antibodies. *Am J Physiol* 269:C1496–C1505.